Switchable Quantum Anomalous Hall State in a Strongly Frustrated Lattice Magnet

Jörn W. F. Venderbos,[1] Maria Daghofer,[1] Jeroen van den Brink,[1] and Sanjeev Kumar[2]
[1]IFW Dresden, P. O. Box 27 01 16, D-01171 Dresden, Germany
[2]Indian Institute of Science Education and Research (IISER) Mohali, Knowledge city, Sector 81, Mohali 140306, India
(Received 17 February 2012; published 18 October 2012)

We establish that the interplay of itinerant fermions with localized magnetic moments on a checkerboard lattice leads to magnetic flux phases. For weak itineracy the flux phase is coplanar and the electronic dispersion takes the shape of graphenelike Dirac fermions. Stronger itineracy drives the formation of a noncoplanar, chiral flux phase, in which the Dirac fermions acquire a topological mass that is proportional to a ferromagnetic spin polarization. Consequently the system self-organizes into a ferromagnetic quantum anomalous Hall state in which the direction of its dissipationless edge currents can be switched by an applied magnetic field.

DOI: 10.1103/PhysRevLett.109.166405 PACS numbers: 71.27.+a, 71.10.−w, 73.43.−f, 75.10.−b

Introduction.—The study of topologically nontrivial states of matter is one of the hottest topics in present-day condensed-matter physics. Topological states require a theoretical paradigm that goes beyond the concept of global symmetry breaking as laid out by Landau. It is remarkable that the theoretical predictions on the existence of various topologically ordered states have rather swiftly led to the discovery of an entirely new class of materials, the topological insulators [1–4]. Recent pioneering experiments have confirmed the key signatures of nontrivial topology in certain materials, e.g., spin-momentum-locked undoubled Dirac fermions [5–7] and the quantum spin Hall effect [8]. These topological insulators are time-reversal-invariant generalizations of the first, much older, topological state of matter, the famous integer quantum Hall states [9,10] that are induced by a magnetic field, which obviously breaks time-reversal (TR) symmetry.

In a seminal work in 1988, Haldane established that a magnetic field is not required to induce states with the same topology as integer quantum Hall states [11]. It was shown that adding complex hopping to a graphenelike Hamiltonian for electrons on a honeycomb lattice opens up topologically nontrivial gaps at the Dirac points, which yields a topologically ordered, insulating state, referred to as a quantum anomalous Hall (QAH) state. An important feature of QAH states are edge channels, in which current can run only in one direction. This is in contrast to quantum spin Hall states, where each edge has two channels carrying currents in opposite directions, one for each spin [12]. QAH states would thus allow very robust, dissipationless charge transport along edge channels, as backscattering would be completely suppressed. However, while signatures of QAH behavior have been reported in some compounds [13–15], the only QAH state so far reported has very recently been realized in 'molecular graphene,' a nanostructure tailored to this purpose [16]. Other approaches suggested so far are spin-orbit-coupled magnetic semiconductors [17], spin-orbit-coupled ad-atoms on graphene [18], or spin-polarized quantum spin Hall states [12].

The experimental difficulty is mirrored by the frailty of theoretical mass-generating mechanisms for a graphene-like kinetic energy with a linear dispersion at the Fermi level. TR-symmetry breaking via (magnetic) order requires rather specific and strong longer-range Coulomb interactions [19], because the Dirac cones' vanishing density of states at the Fermi level renders interaction-driven ordered states energetically less favorable. QAH states can more readily be induced in models with a finite density of states [20–22], especially in cases of quadratic band crossings [23], as for instance found in the checkerboard lattice, which exhibit a weak-coupling instability [23–25].

We will show here that the ground state of itinerant electrons strongly coupled to localized spins on a checkerboard lattice is given by massless Dirac fermions or by a chiral QAH state, depending on parameters. The spin texture underlying the QAH state has a net ferromagnetic (FM) moment, flipping the FM polarization therefore allows us both to induce the QAH state from Dirac fermions and to switch between ground-states of opposite chirality. This possibility to control an edge current by an external magnetic field is an attractive feature in the context of spintronics.

The itinerant checkerboard lattice magnet.—We model the itinerant electrons coupled to localized core spins by a one-band double-exchange model with a competing antiferromagnetic (AFM) superexchange interaction,

$$\hat{H} = -\sum_{\langle ij\rangle}(t_{ij}\ \psi_i^\dagger \psi_j + \text{H.c.}) + \mathrm{J_{AFM}}\sum_{\langle ij\rangle}\mathbf{S}_\mathrm{i}\cdot\mathbf{S}_\mathrm{j}, \qquad (1)$$

where $\psi_i^\dagger$ (ψ_i) creates (annihilates) a fermion on site i. Our discussion will for simplicity first focus on infinite Hund's rule perfectly aligning the fermion spin to the localized spins $\mathbf{S}_i$, but the main results remain valid for finite and even weak coupling, as discussed later. We

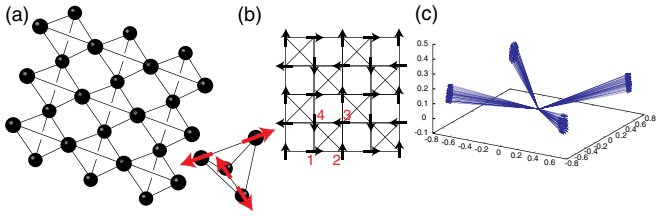

FIG. 1 (color online). (a) Shows the arrangement of tetrahedra that gives rises to the hopping topology of the checkerboard lattice. Spins of the flux phase in the tetrahedral unit cell are also shown. (b) Ordered pattern of spins in the coplanar flux phase represented on the projected checkerboard lattice. (c) Representation of the spins in the "umbrella" spin-chiral state, as obtained with MCMC + optimization for a 16×16 lattice with $J_{\mathrm{AFM}} = 0.105$, where $\delta = 0.148$ compared to 0.141 as would be expected analytically; all spins have been translated to a single site.

investigate here the checkerboard lattice, shown in Fig. 1(b), whose first Brillouin zone is given by $(k_x, k_y) \in \{|k_x + k_y| \leq \pi\} \cap \{|k_x - k_y| \leq \pi\}$. Both "straight" and "diagonal" edges are here included in the sum over $\langle ij \rangle$. This equivalence of the bonds arises when the checkerboard lattice is seen as reflecting the hopping topology of connected tetrahedra, see Fig. 1(a). Since such tetrahedra are building blocks in various frustrated structures, e.g., the pyrochlore lattice of quasi-one-dimensional compounds [26], understanding their frustration is of high interest. We have verified that the results remain intact for weaker "diagonal" hoppings. Stronger diagonal hopping favors a Néel-type ordering, where the electron-spin system decouples into one-dimensional diagonal chains with van Hove singularities at the band edges.

In the absence of charge carriers or for strong AFM coupling $J_{\mathrm{AFM}} \rightarrow \infty$, the Heisenberg term dominates. It can be rewritten in terms of the total spins on the crossed plaquettes $\mathbf{S}_{\mathcal{P}} = \mathbf{S}_1 + \mathbf{S}_2 + \mathbf{S}_3 + \mathbf{S}_4$, giving $J_{\mathrm{AFM}} \sum_{\langle ij \rangle} \mathbf{S}_i \cdot \mathbf{S}_j = (J_{\mathrm{AFM}}/2) \sum_{\mathcal{P}} \mathbf{S}_{\mathcal{P}} \cdot \mathbf{S}_{\mathcal{P}} - J_{\mathrm{AFM}} N$, where N is the number of sites. Clearly, the lowest energy is obtained whenever $\mathbf{S}_{\mathcal{P}} = \mathbf{0}$ for all crossed plaquettes. Since a macroscopic number of configurations fulfill these *local* constraints, the ground-state manifold is highly degenerate. For Ising spins, these local constraints, $\mathbf{S}_{\mathcal{P}} = \mathbf{0}$, are equivalent to the requirement of "two-up–two-down" spins on each crossed plaquette [27]. This is akin to the "two-in–two-out" rule, the ice rule, that governs the magnetic energetics in three-dimensional spin-ice systems, which remain disordered down to the lowest temperatures. The spin-ice rule $\mathbf{S}_{\mathcal{P}} = \mathbf{0}$ on the checkerboard leads to an even larger class of ground states, if Heisenberg spins instead of Ising spins are considered, as is the case in the present Letter.

Doping with itinerant charge carriers can (partly) lift the macroscopic degeneracy of the ground-state manifold [28] because the kinetic energy competes with the ice-rule constraints due to the double-exchange mechanism: For classical on-site spins (with $|\mathbf{S}_i| = 1$), which are specified by polar and azimuthal angles (θ_i, ϕ_i), the effective hopping amplitude is modified by the relative spin orientation as $t_{ij} = t[\cos(\theta_i/2)\cos(\theta_j/2) + \sin(\theta_i/2) \times \sin(\theta_j/2) e^{-i(\phi_i - \phi_j)}]$ [29], where the bare hopping amplitude t is our unit of energy. For the uniform ferromagnet, the electronic bands correspond to those of spinless free fermions on the checkerboard, given by $E_+ = 2t$ and $E_- = -2t - 4t \cos k_x \cos k_y$; the density of states (DOS), $D(\omega) = \langle \frac{1}{N} \sum_k \delta(\omega - \epsilon_k) \rangle$, is shown in Fig. 2(a). In this Letter, we consider here the average density of one electron per two sites, where the kinetic energy has the strongest impact. We use Markov-chain Monte Carlo simulations to anneal the classical spins, where the probability of a spin configuration is given by the free energy of the effective fermionic Hamiltonian, as obtained by exact diagonalization [29]. We have performed calculations on lattices with $N = 8^2$, 12^2, 16^2, and 20^2 sites. Markov-chain Monte Carlo calculations were supplemented with an energy optimization in order to suppress thermal fluctuations [30] and complemented by an analytic weak-coupling analysis.

Massless Dirac fermions through lifting of the spin-ice degeneracy.—For large superexchange coupling $J_{\mathrm{AFM}} \gg 1$, the magnetic order is expected to belong to the highly degenerate ground-state manifold fulfilling $\mathbf{S}_{\mathcal{P}} = \mathbf{0}$. Our Markov-chain Monte Carlo calculations show that the kinetic energy lifts this degeneracy completely and picks out the particular coplanar, but noncollinear, state that is schematically depicted in Fig. 1(b). Nondiagonal bonds connect orthogonal spins, while diagonal bonds connect AFM spins, effectively excluding them from the hopping term. Going around a square plaquette, the electrons pick up a phase $e^{i\pi}$, corresponding to an invariant flux of π, and this special "flux" phase has been shown to arise in models for high-Tc superconductors [31,32] and in the double-exchange models on the square lattice [33–36]. On the unfrustrated square lattice, it competes with the Néel state

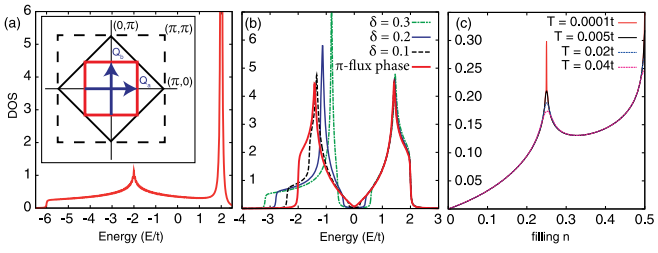

FIG. 2 (color online). Electronic density of states of (a) the FM (spinless) phase, (b) the "flux" phase (in red) and spin-chiral umbrella phase for various δ (see text). The inset of (a) shows the Brillouin zone (black solid) and the Fermi surface (red solid) of the noninteracting checkerboard lattice at quarter filling. The two vectors $\mathbf{Q}_a = (\pi, 0)$ and $\mathbf{Q}_b = (0, \pi)$ perfectly nest the Fermi surface. (c) Spin susceptibility $\chi_0(\mathbf{Q}_a) = \chi_0(\mathbf{Q}_b)$ for various temperatures.

for strong J_{AFM} [33–35], but since it fulfills the ice-rules, it remains stable for $J_{\mathrm{AFM}} > 0.12$ on the checkerboard lattice.

The DOS of the flux phase shows semimetallic behavior [see Fig. 2(b)] that originates from two Dirac points in the spectrum. Low-energy excitations are described by a relativistic Dirac equation, in full analogy with graphene [37]. The core-spin texture $\Lambda_i = (\theta_i, \phi_i)$ of the flux phase can be written as $\Lambda_i = (\pi/2, (i-1)\pi/2)$ with $i = 1, 2, 3, 4$ [see Fig. 1(a)]. Even though the magnetic texture has a four-site unit cell, the two-site electronic unit cell need not be enlarged. The electronic Hamiltonian, in the $(\psi_A^\dagger, \psi_B^\dagger)$ basis, is then given by $H(\boldsymbol{k}) = \boldsymbol{d}(\boldsymbol{k}) \cdot \boldsymbol{\sigma}$, with the Pauli matrices $\boldsymbol{\sigma} = (\sigma^x, \sigma^y, \sigma^z)$ and $\boldsymbol{d}(\boldsymbol{k}) = -(\cos k_x + \cos k_y, \cos k_x - \cos k_y, 0)$, the band structure of which is shown in Fig. 3(a). The two inequivalent Dirac points, or valleys, are located at $\boldsymbol{M}_\pm = (\pm\pi/2, \pi/2)$.

Massive QAH Dirac fermions.—Having established that the electronic kinetic energy selects a unique noncollinear pattern for the checkerboard double-exchange magnet, which has a graphenelike Dirac spectrum, we consider next what happens upon an increase of the itineracy. Lowering J_{AFM}, we find that the magnetic interactions

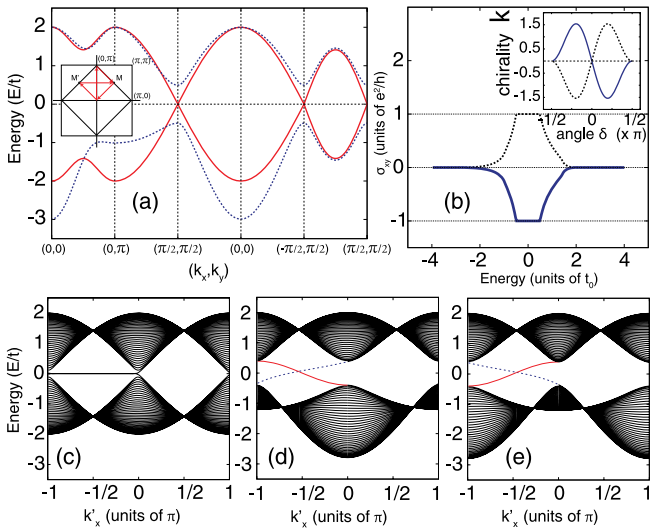

FIG. 3 (color online). (a) The band structure of the gapless flux phase (red) and the insulating chiral phase (blue, $\delta = 0.3$) along a path in the Brillouin zone specified in the inset. (b) Quantized Hall conductivity in the chiral state ($\delta = 0.3$), when the Fermi level is in the gap, the quantized value depends on the chirality of the spin state. The inset shows the calculated chirality of the states $\Lambda^\pm$, where the dashed (solid) line corresponds to $+$ ($-$). ($c-e$) Spectrum of the flux phase calculated for a strip geometry, which explicitly shows the edge states at the open boundary. (c) π-flux phase ($\delta = 0.0$) exhibits edge states similar to graphene. (d),(e) Chiral gapped phase ($\delta = 0.2$); chiral edge states connect valence and conduction bands. The states drawn with solid (dashed) lines lives on the top (bottom) edge. The chirality in (e) is reversed with respect to (d), the right- and left-moving states are consequently exchanged.

enforcing the tetrahedron rules are overcome by the electronic kinetic energy for $J_{\mathrm{AFM}} \lesssim 0.12$. The transition is continuous and can be understood as a tilting of the flux pattern out of the plane, forming an "umbrella". An example is shown in Fig. 1(c): the spins fall along four directions, whose projections onto the x-y plane mirror the "π-flux"-phase pattern, but there is an additional FM component along the z axis. The spins can be described using an Ising variable $s = \pm 1$ (which will turn out to correspond to a scalar spin chirality) and a continuous parameter δ giving the tilting along $\mp z$: $\{\Lambda_i^s(\delta)\} = (\pi/2 + \delta, s(i-1)\pi/2)$, where $i = 1, 2,3,4$ again runs around a crossed plaquette. A similar scenario, but with an 8-site unit cell and Chern numbers ± 2, arises on a square lattice with longer-range couplings when nearest-neighbor hoppings are strongly modulated [36].

The scalar spin chirality of the state is defined as $\kappa = \sum_{\mathcal{T}} \mathbf{S}_i \cdot \mathbf{S}_j \times \mathbf{S}_k$, where the sum is over all triangles $\mathcal{T}$ of the checkerboard lattice, and $\mathbf{S}_i \cdot \mathbf{S}_j \times \mathbf{S}_k$ is taken in the counter-clockwise direction. The chirality as a function of δ is plotted in the inset of Fig. 3(b) for umbrella states $\Lambda^\pm$, it is $\kappa \approx -s\delta$ for small δ. The label $\pm s$ decides the sign of the chirality for $\delta > 0$ and is related to a (counter) clockwise rotation of the spin projection onto the x-y plane. The umbrella states, in addition to a continuous spin rotation symmetry, thus also break a discrete $\mathbb{Z}_2$ symmetry. As a discrete symmetry can also be broken at finite temperature in 2D, chiral ordering may be possible even without long-range magnetic ordering [38].

Tilting the spins breaks TR symmetry for the electronic degrees of freedom, as fluxes through elementary plaquettes are related to the solid angle subtended by the spins surrounding the plaquette. Calculating the hoppings in the umbrella states, we find that hopping on the straight bonds is given by $t_1^s = e^{-si\pi/4}(1 - si\sin\delta)/\sqrt{2}$, with $|t_1^s| = \sqrt{(1+\sin^2\delta)/2} \equiv t_1$ and $\phi_1^s = \arctan(-s\sin\delta) - s\pi/4 \equiv \phi^s$ [see Fig. 1(c)]. In addition, hopping along the diagonal bonds is no longer 0 but $t_2 = -\sin\delta$, independent of chirality. This leads us to the effective electronic Hamiltonian

$$
\begin{aligned}
&H^s(\boldsymbol{k}) = \boldsymbol{d}(\boldsymbol{k}) \cdot \boldsymbol{\sigma} + d^0(\boldsymbol{k})\sigma^0, \quad \text{with} \\
&d^0(\boldsymbol{k}) = -2t_2 \cos k_x \cos k_y,\ d^3(\boldsymbol{k}) = 2t_2 \sin k_x \sin k_y, \\
&d^1(\boldsymbol{k}) = -2t_1 \cos\phi^s(\cos k_x + \cos k_y), \quad \text{and} \\
&d^2(\boldsymbol{k}) = -2t_1 \sin\phi^s(-\cos k_x + \cos k_y),
\end{aligned}
\tag{2}
$$

where the two states referred to by the matrices are again the two sites of the unit cell and σ^0 is the unit matrix so that the Dirac Hamiltonian above is recovered for $\delta = 0$, implying $\phi^s = \pi/4$ and $t_2 = 0$. From the DOS [Fig. 2(b)] and the band structure [Fig. 3(a)], it is clear that finite $\delta \neq 0$ opens a gap for the Dirac cones. Since the hoppings are complex and the diagonal bonds have been activated, both TR and parity symmetries are broken, allowing a QAH

state [39]. To establish that the gapped state is indeed topologically nontrivial, we calculate the Chern number of the occupied band (for a general band n $C_n = \frac{1}{2\pi i} \times \oint_{\partial \mathrm{BZ}} d\boldsymbol{k} \cdot \boldsymbol{A}(\boldsymbol{k})$, where $\boldsymbol{A}(\boldsymbol{k}) = \langle n\boldsymbol{k}|\nabla_{\boldsymbol{k}}|n\boldsymbol{k}\rangle$ is the Berry connection) and find $C = \mathrm{sgn}(t_2)\mathrm{sgn}(\sin 2\phi^s)$. Chirality and Chern number hence perfectly correlate and we observe that inverting the magnetic polarization $\delta \to -\delta$ flips both the spin chirality and the Chern number. The off-diagonal Hall conductivity as a function of chemical potential, obtained from Eq. (2) for $\delta = 0.3$, is shown in Fig. 3(b). Figures 3(c)–3(e) show the effect of nontrivial topology on the edge of the system: chiral edge states connect valence and conduction band. As can be seen by comparing Figs. 3(d) and 3(e), the direction of the edge currents can be reversed by inverting the spin chirality. Particularly appealing would be a system with a ground state still in the ''massless'' flux phase, but close to the transition to the QAH state, where a topological gap could be opened by a small magnetic field, and the direction of the edge currents could be manipulated by its orientation.

The observation that spin configurations of the umbrella states are continuously connected to the coplanar flux phase suggests that the electronic QAH state can be understood from the low-energy physics of the electrons at the Dirac points. In general, when the low-energy electronic theory is described by two inequivalent Dirac fermions there are four possible mass terms that may gap out the spectrum [40]. Three of those are compatible and correspond to a one-component charge density wave instability (sublattice potential) parameter and a two-component bond-density wave instability. The fourth possibility to open a gap is a time-reversal symmetry breaking perturbation. The latter case applies to the present situation, in full correspondence with the original proposal for the graphene lattice [11,41].

Weak Hund's rule coupling.—Up to this point we have studied the Hamiltonian in Eq. (1), which assumes a very strong coupling between localized and itinerant electronic spins. We now briefly touch on the case where this Hund's rule coupling is arbitrary and possibly weak. This situation is generically described by the Kondo lattice model (more details in Ref. [41]), where itinerant spinful electrons are coupled to a classical spin field,

$$\hat{H} = -t \sum_{\langle ij\rangle,\alpha} (\psi^{\dagger}_{i\alpha}\psi_{j\alpha} + \mathrm{H.c.}) - \mathrm{J_H} \sum_{\mathrm{i}} \mathbf{S}_{\mathrm{i}} \cdot \psi^{\dagger}_{\mathrm{i}\alpha} \boldsymbol{\sigma}_{\alpha\beta} \psi_{\mathrm{i}\beta}, \tag{3}$$

where the vector of Pauli matrices $\boldsymbol{\sigma}_{\alpha\beta}$ refers to the spin of the itinerant electrons. Half filling in the spinless case corresponds to quarter filling in the spinful case, where the Fermi surface (FS) of free fermions on the checkerboard lattice is a square, as shown in the inset of Fig. 2(a), and where the DOS shows a van Hove singularity, see main panel of Fig. 2(a). Two ordering vectors $\mathbf{Q}_a = (\pi, 0)$ and $\mathbf{Q}_b = (0, \pi)$ perfectly nest the FS and the order parameter of the gapped and gapless flux phases can be written as $\mathbf{S}(\mathbf{r}_i) = [\mathcal{S}_a \cos(\mathbf{Q}_a \cdot \mathbf{r}_i), \mathcal{S}_b \cos(\mathbf{Q}_b \cdot \mathbf{r}_i), \mathcal{S}_c]$, with the conditions $|\mathcal{S}_a| = |\mathcal{S}_b|$ and $\mathcal{S}_a^2 + \mathcal{S}_b^2 + \mathcal{S}_c^2 = 1$. The gapless flux phase with Dirac points corresponds to $\mathcal{S}_c = 0$. The Ruderman-Kittel-Kasuya-Yosida interaction mediated by the electrons between the spins is given by $\Omega^{(2)} = -J_H^2 \sum_{\boldsymbol{p}} \chi_0(\boldsymbol{p}) S^{\alpha}(-\boldsymbol{p}) S^{\alpha}(\boldsymbol{p})$ and is thus determined by the spin susceptibility $\chi_0(\boldsymbol{p}) = -\sum_n \sum_{\boldsymbol{k}} \mathrm{Tr}[\hat{G}_0(\boldsymbol{k}, i\omega_n) \times \hat{G}_0(\boldsymbol{k}+\boldsymbol{p}, i\omega_n)]/(2N)$, where $\hat{G}_0(\boldsymbol{k}, i\omega_n)$ is the noninteracting electronic Green's function. The temperature dependence of $\chi_0(\pi, 0)$ and $\chi_0(0, \pi)$ is shown in Fig. 2, clearly showing divergent behavior at quarter filling. Comparison with alternatively ordered states is presented in Ref. [41]. We conclude that the double-q ordered flux phase is expected to be stabilized by weak-coupling instability connected to FS nesting. Additional AFM coupling between the localized spins in the spinful model of Hamiltonian (3) enhances the energetic stability of the gapped and gapless flux phases with respect to the ferromagnet.

Discussion and conclusions.—In conclusion, we investigated the interplay of itinerant electrons with a frustrated AFM spin background on the checkerboard lattice using Monte Carlo methods and analytic approaches. The electron kinetic energy selects a unique magnetic ground state, the π-flux phase, from the macroscopically degenerate *spin-ice* manifold optimizing the AFM interactions. Its electronic states feature massless Dirac fermions. Both a magnetic field and slightly stronger kinetic energy can induce a spin chirality, from which the Dirac fermions inherit a topologically nontrivial mass.

The Kondo-lattice model on the checkerboard model thus provides a direct realization of Haldane's proposal for obtaining a QAH state [11]. QAH states on the checkerboard lattice have also been proposed as candidates for hosting an anomalous *fractional* quantum-Hall-like state [24,42,43]. This requires nearly dispersionless bands; in the present scenario, additional longer-range hopping $-2t_3(\cos 2k_x + \cos 2k_y)$ can give a ratio of band gap vs band width of ≈ 5 for $\delta = 0.3$. While this is considerably less than ratios achievable by tuning all parameters [24] or in t_{2g}-orbital systems [44,45], it is comparable to e_g [44] systems or a square-lattice model [46].

Interestingly, the QAH state's chirality is coupled to a FM spin polarization and the direction of the edge currents can thus be switched by a magnetic field, an alluring property for quantum spintronics applications. Such a magnetic field would also tend to suppress magnetic domains with opposite FM moment and chirality. However, magnetic domains with opposite uniform ferromagnetic components would also be very interesting, because the domain walls separating them are expected to provide one-dimensional chiral transport channels. In addition, recent work has shown that topological defects of the spin texture, e.g., $\mathbb{Z}_2$ vortices, carry electronic midgap states representing fractionally charged excitations [47].

This research was supported by the Interphase Program of the Dutch Science Foundation NWO/FOM (J. V. and J. v. d. B.) and by the Emmy-Noether program of the DFG (M. D.). S. K. acknowledges support from DST, India.

[1] C. L. Kane and E. J. Mele, Phys. Rev. Lett. **95**, 146802 (2005).
[2] R. Roy, Phys. Rev. B **79**, 195322 (2009).
[3] J. E. Moore and L. Balents, Phys. Rev. B **75**, 121306 (2007).
[4] L. Fu, C. L. Kane, and E. J. Mele, Phys. Rev. Lett. **98**, 106803 (2007).
[5] Y. Xia, L. Wray, D. Qian, D. Hsieh, A. Pal, H. Lin, A. Bansil, D. Grauer, Y. S. Hor, R. J. Cava, and M. Z. Hasan, arXiv:0812.2078.
[6] D. Hsieh, Y. Xia, D. Qian, L. Wray, J. H. Dil, F. Meier, J. Osterwalder, L. Patthey, J. G. Checkelsky, N. P. Ong, A. V. Fedorov, H. Lin, A. Bansil, D. Grauer, Y. S. Hor, R. J. Cava, and M. Z. Hasan, Nature (London) **460**, 1101 (2009).
[7] Y. Xia, D. Qian, D. Hsieh, L. Wray, A. Pal, H. Lin, A. Bansil, D. Grauer, Y. S. Hor, R. J. Cava, and M. Z. Hasan, Nature Phys. **5**, 398 (2009).
[8] M. Koenig, S. Wiedmann, C. Bruene, A. Roth, H. Buhmann, L. W. Molenkamp, X.-L. Qi, and S.-C. Zhang, Science **318**, 766 (2007).
[9] K. von Klitzing, G. Dorda, and M. Pepper, Phys. Rev. Lett. **45**, 494 (1980).
[10] D. J. Thouless, M. Kohmoto, M. P. Nightingale, and M. den Nijs, Phys. Rev. Lett. **49**, 405 (1982).
[11] F. D. M. Haldane, Phys. Rev. Lett. **61**, 2015 (1988).
[12] C.-X. Liu, X.-L. Qi, X. Dai, Z. Fang, and S.-C. Zhang, Phys. Rev. Lett. **101**, 146802 (2008).
[13] Y. Taguchi, Y. Oohara, H. Yoshizawa, N. Nagaosa, and Y. Tokura, Science **291**, 2573 (2001).
[14] Y. Machida, S. Nakatsuji, Y. Maeno, T. Tayama, T. Sakakibara, and S. Onoda, Phys. Rev. Lett. **98**, 057203 (2007).
[15] H. Takatsu, S. Yonezawa, S. Fujimoto, and Y. Maeno, Phys. Rev. Lett. **105**, 137201 (2010).
[16] K. K. Gomes, W. Mar, W. Ko, F. Guinea, and H. C. Manoharan, Nature (London) **483**, 306 (2012).
[17] X.-L. Qi, Y.-S. Wu, and S.-C. Zhang, Phys. Rev. B **74**, 085308 (2006).
[18] H. Zhang, C. Lazo, S. Blügel, S. Heinze, and Y. Mokrousov, Phys. Rev. Lett. **108**, 056802 (2012).
[19] S. Raghu, X.-L. Qi, C. Honerkamp, and S.-C. Zhang, Phys. Rev. Lett. **100**, 156401 (2008).
[20] I. Martin and C. D. Batista, Phys. Rev. Lett. **101**, 156402 (2008).
[21] S. Kumar and J. van den Brink, Phys. Rev. Lett. **105**, 216405 (2010).
[22] K. Ohgushi, S. Murakami, and N. Nagaosa, Phys. Rev. B **62**, R6065 (2000).
[23] K. Sun, H. Yao, E. Fradkin, and S. A. Kivelson, Phys. Rev. Lett. **103**, 046811 (2009).
[24] K. Sun, Z. Gu, H. Katsura, and S. Das Sarma, Phys. Rev. Lett. **106**, 236803 (2011).
[25] S. Uebelacker and C. Honerkamp, Phys. Rev. B **84**, 205122 (2011).
[26] P. Schobinger-Papamantellos, J. Rodríguez-Carvajal, and K. H. J. Buschow, J. Magn. Magn. Mater. **310**, 63 (2007).
[27] L. D. C. Jaubert, M. Haque, and R. Moessner, Phys. Rev. Lett. **107**, 177202 (2011).
[28] L. D. C. Jaubert, S. Piatecki, M. Haque, and R. Moessner, Phys. Rev. B **85**, 054425 (2012).
[29] E. Dagotto, T. Hotta, and A. Moreo, Phys. Rep. **344**, 1 (2001).
[30] R. Yu, S. Yunoki, S. Dong, and E. Dagotto, Phys. Rev. B **80**, 125115 (2009).
[31] I. Affleck and J. B. Marston, Phys. Rev. B **37**, 3774 (1988).
[32] J. Lorenzana, G. Seibold, C. Ortix, and M. Grilli, Phys. Rev. Lett. **101**, 186402 (2008).
[33] M. Yamanaka, W. Koshibae, and S. Maekawa, Phys. Rev. Lett. **81**, 5604 (1998).
[34] D. F. Agterberg and S. Yunoki, Phys. Rev. B **62**, 13816 (2000).
[35] H. Aliaga, B. Normand, K. Hallberg, M. Avignon, and B. Alascio, Phys. Rev. B **64**, 024422 (2001).
[36] X. Chen, S. Dong, and J. M. Liu, Phys. Rev. B **81**, 064420 (2010).
[37] A. H. Castro Neto, F. Guinea, N. M. R. Peres, K. S. Novoselov, and A. K. Geim, Rev. Mod. Phys. **81**, 109 (2009).
[38] Y. Kato, I. Martin, and C. D. Batista, Phys. Rev. Lett. **105**, 266405 (2010).
[39] M. Onoda and N. Nagaosa, J. Phys. Soc. Jpn. **71**, 19 (2002).
[40] S. Ryu, C. Mudry, C.-Y. Hou, and C. Chamon, Phys. Rev. B **80**, 205319 (2009).
[41] See Supplemental Material at http://link.aps.org/supplemental/10.1103/PhysRevLett.109.166405 for details of the weak-coupling theory, including susceptibility calculations, and details of the low-energy Dirac theory of the gapped chiral phase.
[42] D. N. Sheng, Z.-C. Gu, K. Sun, and L. Sheng, Nature Commun. **2**, 389 (2011).
[43] N. Regnault and B. Bernevig, Phys. Rev. X **1**, 021014 (2011).
[44] J. W. F. Venderbos, M. Daghofer, and J. van den Brink, Phys. Rev. Lett. **107**, 116401 (2011).
[45] J. W. F. Venderbos, S. Kourtis, J. van den Brink, and M. Daghofer, Phys. Rev. Lett. **108**, 126405 (2012).
[46] T. Neupert, L. Santos, C. Chamon, and C. Mudry, Phys. Rev. Lett. **106**, 236804 (2011).
[47] R. A. Muniz, A. Rahmani, and I. Martin, arXiv:1112.3347 (2011).